

Lasers in Manufacturing Conference 2021

# A measuring system based on chromatic confocal displacement sensor integrated with laser head for monitoring of laser metal deposition process

Piotr Koruba<sup>a,\*</sup>, Adrian Zakrzewski<sup>a</sup>, Piotr Jurewicz<sup>a</sup>, Michał Ćwikła<sup>a</sup>, Jacek Reiner<sup>a</sup>

<sup>a</sup>Wrocław University of Science and Technology, Wybrzeże Wyspiańskiego 27, Wrocław 50-370, Poland

---

## Abstract

The measurement of geometrical properties of a sample during laser material processing is still an open research issue. Thus, the knowledge about the laser focus in relation to sample before, during and after the process is considered as one of the most crucial parameters. In this study, we indicate that the chromatic confocal displacement sensor integrated with laser head can serve as an alternative for current solutions used in monitoring of laser metal deposition process. Therefore, the design procedures of measuring system is described, consisting in numerical modelling, selection of system components. Moreover, in order to determine the functionality parameters of the system it was experimentally characterized in two regimes i.e. off-line and on-line (with and without presence of laser beam, respectively). Additionally, the various methods for spectral data processing were presented. Finally, the preliminary measurement results obtained with the measuring system during laser metal deposition were presented and discussed.

Keywords: laser metal deposition, chromatic aberration, optical system design,

---

## 1. Introduction

Laser Metal Deposition (LMD) is a widely used laser processing technology for application such as deposition of functional coatings, repair of used machine parts and additive manufacturing from digital models. In this process laser beam creates a melt pool on the surface on the substrate, where the additional material is added and melts creating single clad. From many process parameters one of the most crucial for process stability is

---

\* Corresponding author. Tel.: +48-71-320-4635 .  
E-mail address: piotr.koruba@pwr.edu.pl

stand-off – the distance between the cladding nozzle and the substrate or already deposited clad. Not only is this parameter important in case of volume build-up, but also when multilayer coating is being deposited. Currently there is a common method for stand-off determination using distance patterns, yet it works only in case of single clad, since it is preprocess operation. Unfortunately, the height of deposited layer can vary greatly because of the impact of other process, powder or substrate parameters. Therefore an in-situ measurement is needed to perform appropriate motion with the laser head in the direction of the build-up. Several systems has been already developed for measuring displacement/distance in laser material processing.

One of the approaches to measure deposited clad height so as to deliver this information to process controller was presented by Mazumder et al., 2000 and Song et al., 2012. That systems consisted of three CCD cameras located at 120° spacing in horizontal plane and at 45° angle to the axis of the laser beam. Another method is to predict the cladding height based on melt pool properties such as width or shape, that can be acquired using single CCD camera (Hu et al., 2003) or a trinocular system (Asselin et al., 2005).

In case of distance sensor based on triangulation the system consists of a low power laser that generates a spot or a line onto the object and acquisition device (e.g. CCD camera), that acquires images of the projection and subsequently the distance to the object feature is determined based on the calculated angles and distances of the measurement setup. Most of the developed systems are limited to offline measurements of process results like inspection of the geometry of welded joints (Huang and Kovacevic, 2011).

On the other hand, Donadello et al., 2018 proposed coaxial triangulation system for height monitoring in LMD process. This system was fully integrated into the laser head and utilized green laser light, that was registered on the CCD camera after being scattered on the cladged object. In order to make the measurement robust, the system was equipped also with diaphragm and selected band-pass filter positioned in front of camera.

Another alternative might be LCI (Low Coherence Interference) based sensors. Authier et. al, 2016 presented the use of the commercial IDM (In-process Depth Meter) system developed by PRECITEC for measuring the depth of the capillary in keyhole laser welding. This solution is composed of Michelson interferometer attached to the laser head, spectrometer and linear CCD sensor. The output signal from the interferometer contains oscillations describing the difference in optical paths between reference and measuring arm. Moreover, Neef et. al., 2014 used the IDM system to develop a sensor embedded into the SLM system (Selective Laser Melting). The authors indicated the possible application of this sensor such as: inspection of powder bed, determination of the focus position or monitoring of the melt pool. However in their work only the characterization of melted surface was presented. DePond et. al., 2018 implemented LD-600 (Kingston) LCI sensor to SLM system for SD-OCT (Spectral-Domain Optical Coherence Tomography). The aim of the study was to measure layer roughness during after the fusion within SLM process. Furthermore, actual commercial devices are not designed for the conditions of the LC process and they need additional protection from heated powder particles and process laser light scattering.

In this study, it is indicated that the chromatic confocal displacement sensor integrated with a laser head can be regarded as competitive solution for measuring clad height in LMD process. The operation of the proposed sensor is based on the phenomenon of longitudinal chromatic aberration, which is widely used in case of stand-alone measurement systems. However, integrating such a system with the laser optics is a novelty. Such a measurement system can work in both off-line (pre- or post-process) or on-line (in-process) regime. The main aspect of this paper is to show the workflow of developing measurement system for laser metal deposition process. Therefore, the process of designing the optical system is presented, followed by its characterization, description of spectral data processing as well as validation in off-line and on-line regimes.

## 2. Development of measurement system

### 2.1. Measurement system based on longitudinal chromatic aberration phenomenon

Commonly used stand-alone chromatic sensors are based on a system of two chromatic lenses ( $ASH_1$ ,  $ASH_2$ ) that are spaced less than the sum of their back focal lengths (BFL). Consequently, the focusing of the sensor operating point is achieved behind the second lens. In the case of the achromatic system, integrated with the optical system of the laser head (Fig. 1), the working point is determined by the processing lens (LL) of the head, which is usually characterized by a large effective focal length. Therefore, the orientation of the two chromatic lenses is modified to obtain an "infinity image" for central wavelength ( $\lambda_{cen}$ ) behind the chromatic system

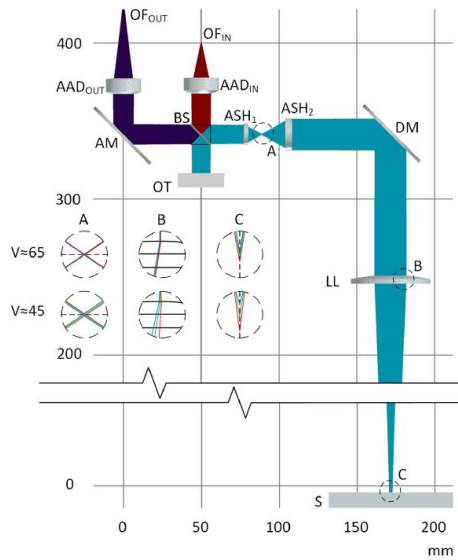


Fig. 1. The principle of operation in case of confocal displacement sensor integrated within optical laser head (Zakrzewski et al., 2020)

Coupling/uncoupling of the beam to the receiving optical fiber/from the sending optical fiber is performed by aspherical achromatic doublets ( $AAD_{out}/AAD_{in}$ ), allowing for the level reduction of additional aberrations in the system, and as a result, the possibility of more precise control of the designed lateral chromatic aberration (LCA) range, which in this case depends only on the value of the chromatic aberration shown by the  $ASH_1$  and  $ASH_2$  lenses. Additionally, all modeled lenses (excluding LL) were spherical aberration corrected. This disadvantage has a negative impact onto the obtained intensity (I) and full width at half maximum (FWHM) value of the spectral peak of interest. The use of  $ASH_1$  and  $ASH_2$  aspherical lenses is aimed at increasing the effect of chromatic aberration and, consequently, ensuring the desired measuring range of the sensor. Commonly, these types of lenses are made of the following materials: D-ZK3, D-ZLaF52LA, H-LaK54 and S-LAH64. When selecting optical elements for the system, one should be guided by the selection of elements that have favorable reflection/transmission characteristics for the wavelength range, which the sensor works on, at the same time taking into account the high transmissions for the laser beam of the dichroic mirror (DM) and LL components.

## 2.2. Design of measurement system based on numerical analysis

The main purpose of the numerical analysis was to define the optical elements of the optical system so as to obtain the highest possible resolution (low FWHM value), the LCA value desired by the user, and the highest possible system efficiency (high  $I$  value). Maximizing the value of the radiation intensity of the measuring beam returning to the detector is important from the perspective of measuring the displacement against highly scattering or absorbing materials. On the other hand, from the perspective of laser processes, the maximization of the radiation intensity value of the measuring beam is of particular importance for on-line measurements (during the process of heating the material with a laser beam).

In order to accomplish this task, the authors proposed a methodology for numerical analysis that divides the selection of system components into three sections (Fig. 2) Each section is subjected to the qualitative assessment of QS parameter, i.e. the arithmetic mean of the component indicators ( $Q_{LCA}$ ,  $Q_{Igeo}$ ,  $Q_{FWHM}$ ).

For considerations of the developed methodology, the authors proposes the use of software for geometric optics (WinLens 3D Basic), which allows the modeling of the entire optical system, taking into account the position of elements in relation to each other, as well as spectral characteristics and anti-reflection coatings. The selection of optical components can be based on commercially available or custom components in order to obtain an unique relationship between the range of aberration, the efficiency of the system and its resolution. The authors suggest using aspherical lenses to avoid introducing unwanted aberrations into the optical system, thus improving the quality of the system.

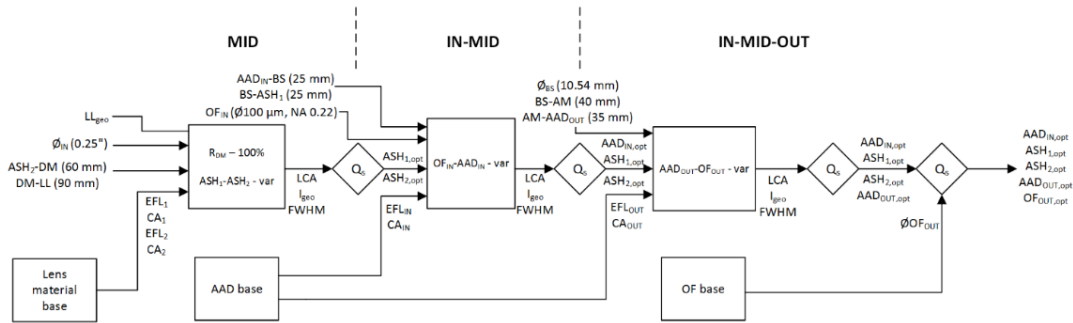


Fig. 2. The diagram showing the methodology for optimization of optical system during numerical analysis (Zakrzewski et al., 2020)

The implementation of the proposed methodology begins with the selection of  $ASH_1$  and  $ASH_2$  lenses in the chromatic system and the quantification of their impact on the parameters of interest (MID section). At this step, the presence of a process lens (LL), a dichroic mirror (DM), and the geometrical relationship between the components present are taken into account. In the IN-MID section, the coupling of the measurement beam to the MID section, by  $AAD_{IN}$  is investigated. Moreover, the  $OF_{IN}$  is included in the analysis, as well as the geometrical relations between  $AAD_{IN}$ , BS and  $ASH_1$ . Finally, in the IN-MID-OUT section, the coupling of measurement beam to the  $OF_{OUT}$ . In this section, determination of both  $AAD_{OUT}$  and  $OF_{OUT}$  is carried out, followed by including the constant values of the beam splitter BS size and the geometrical relations between BS, AM and  $AAD_{OUT}$ .

## 2.3. Setup of the experimental stand

The principle of operation of the developed optical system is schematically presented in Fig. 3. The measurement beam is generated by a wide-spectral light source (BLS) and coupled to an optical fiber ( $OF_{IN}$ )

with a core diameter of 100  $\mu\text{m}$  and  $\text{NA} = 0.22$ . In order to increase the efficiency of coupling the measuring beam to the  $\text{OF}_{\text{IN}}$  fiber, a fiber optic (FC) collimator with an effective focal length of 10.92 mm was used. Then, the beam from the front of the  $\text{OF}_{\text{IN}}$  fiber is directed to the aspherical achromatic doublet ( $\text{AAD}_{\text{IN}}$ ) with  $\text{EFL} = 30$  mm. The distance between  $\text{OF}_{\text{IN}}$  and  $\text{AAD}_{\text{IN}}$  has been established in such a way as to ensure that the beam behind the  $\text{AAD}_{\text{IN}}$  is collimated for the central wavelength of the spectral operating range of the optical system ( $\lambda_{\text{cen}} - 575$  nm). Subsequently, the beam is directed to a beam splitter (BS) with a percentage division of 50:50 (R: T). The part of the beam is directed to the optical trap (OT), whereas the reflected part of the beam is focused by the aspherical lens ( $\text{ASH}_1$ ) with  $\text{EFL} = 12$  mm and directed to the second aspherical lens ( $\text{ASH}_2$ ) with  $\text{EFL} = 20$  mm. The measurement beam after passing the  $\text{ASH}_2$  is collimated again for  $\lambda_{\text{cen}}$ . As these lenses are made of the S-LAH64 material characterized by a low Abbe number ( $V = 47.37$ ), the phenomenon of longitudinal chromatic aberration enhancement occurs behind them.

Subsequently, the measuring beam is introduced through the monitoring port to the laser head placed on the Reis RV60-40 robot arm. After reflection from the dichroic filter (DM), the beam is focused on the sample (S) through a processing lens (LL) characterized by  $\text{EFL} = 250$  mm. The value of  $\text{EFL}$  of LL directly defines the distance of the optical system work point (WD). As the repeatability of position setting by the robot arm is at the level of 100  $\mu\text{m}$ , an electronically controlled linear stage is additionally placed under the laser head. It is characterized by a position repeatability of 1.6  $\mu\text{m}$ . Due to this solution, it is possible to characterize the optical system with much greater precision. After reflection from S, the measuring beam propagates again through all components up to BS. This time the transmission beam is used and directed to an aspherical achromatic doublet ( $\text{AAD}_{\text{OUT}}$ ) by reflection from a mirror (AM), the angular positions of which can be adjusted. Finally, the measurement beam is focused by  $\text{AAD}_{\text{OUT}}$  on the fiber front ( $\text{OF}_{\text{OUT}}$ ) with a core diameter of 100  $\mu\text{m}$  and  $\text{NA} = 0.22$ , which is connected to an optical spectrum analyzer representing the high resolution (0.27 nm) HR4000 spectrometer (Ocean Optics). For the characterization of the developed optical system, the material commonly used in laser processing, i.e. austenitic stainless steel AISI 316L, titanium alloy Ti6Al4V and the reference material in the form of a coated silver mirror (PSM) were selected. In case of the latter, it was due to the high and practically constant reflectance value in the spectral operating range of the system.

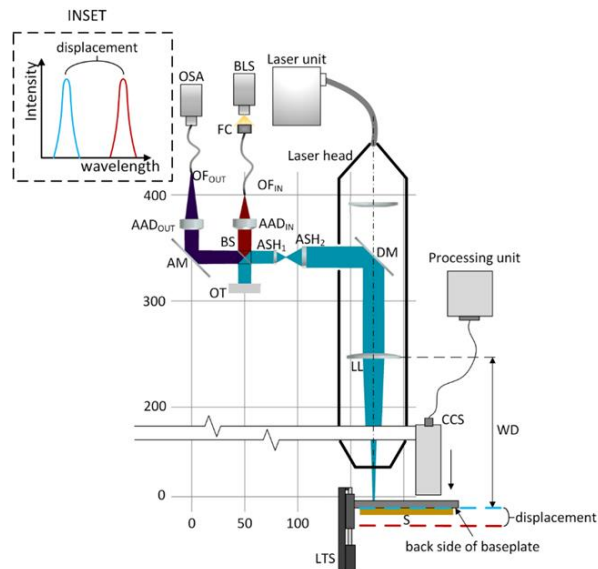


Fig. 3. Schematic view of the developed optical system for distance measurement in LMD process

## 2.4. Spectral data processing

The purpose of the analysis of the spectral data was to propose a specific measure determined on its basis. This measure should first of all offer a high linearity of the sensor characteristic. As exemplary measures, authors proposed the signal maximum argument and the central length of the fitted Gaussian, Lorentzian or Voigt functions. To evaluate the effectiveness of the measures and in order to select the best one, a linear stage with a sample attached to it was placed under the laser head with the sensor. It was used to collect a set of spectrum measurements at different distance between the sample and the laser head. A range of 50 mm was analyzed. Before determining the measures, the spectral signal was limited to the range of 400-800 nm and filtered with a low-pass filter. The fit of the mentioned functions was performed with the use of the Levenberg-Marquardt nonlinear optimization algorithm. The measure in the form of the maximum argument was the fastest algorithm, but also the most susceptible to disturbances. Additionally, the resolution of this measure is directly limited by the resolution of the spectrometer. The Gaussian, Lorentzian, and Voigt fits can increase the accuracy.

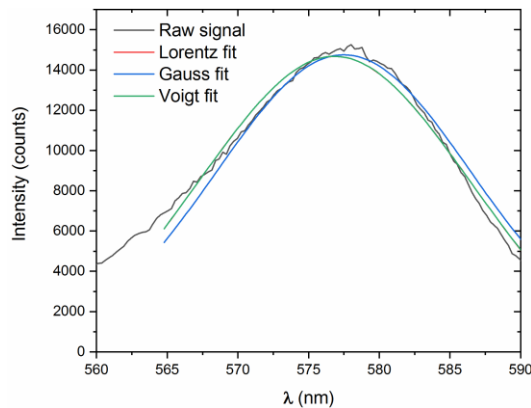


Fig. 4. Results of fitting selected functions to raw signal registered by the system's detector

Based on the collected data, the described measures were determined and the distance-measure characteristics were plotted. The quality of the fit with the mentioned functions was not directly assessed. The effectiveness of the proposed methods was analyzed on the PSM material, which was moved over the full range of the stage, i.e. from 225 to 275 mm from the LL with a 1 mm step. The measurement was carried out 5 times, and after each measurement the sample was disassembled and reassembled. Then, the measured values were averaged. The obtained system calibration curves using various methods are presented in the figure below (Fig. 5). The 0 mm displacement point corresponds to the working distance of the system (250 mm). There is a satisfactory agreement between the curves from experimental measurements and the results of numerical analyzes.

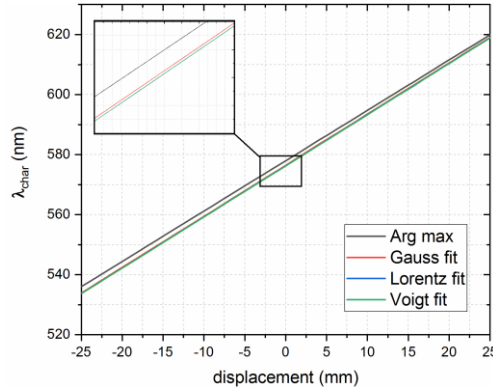


Fig. 5. Optical system calibration curves obtained on the basis of various methods of spectral data processing

### 3. Characterization of the system in the off-line regime

In the first step of the system characterization, the process of its calibration was performed according to the methodology defined by Leach, 2014 for optical displacement sensors. Consequently, the reference value of the displacement was determined based on the indication of the electronically controlled linear stage. The signal registered by the system detector was in the form of a characteristic spectral peak. Its spectral shift is closely related to the displacement of the sample. It enabled creating the so-called system calibration curve.. The system accuracy was determined according to ISO 5725 on the basis of the two parameters: correctness (trueness or bias) and precision.

The correctness of an indication is defined as the maximum discrepancy between the mean value obtained from a series of test results and the adopted reference value. Therefore, it is expressed as the maximum difference between the sample position calculated from the equation of the determined calibration curve (Fig. 5) and the reference value read from the stage used to move the sample.

In the contrary, precision is defined as the degree of agreement between test results and is calculated as the standard deviation of the multiple indications. Therefore, the measurements were carried out as a result of the two-way approach of the stage to the 0 mm displacement position. This procedure was repeated 15 times. Then, the standard deviation of the  $\lambda_{char}$  values extracted by the selected algorithms was determined. Finally, the precision was calculated on the basis of the calibration curve. System resolution is defined as the smallest change in the value of the input parameter (sample displacement) that causes a change in the output signal (extracted  $\lambda_{char}$ ) and was determined in accordance with the methodology presented by Luo et al, 2012. The sample was moved in increments of 2.0  $\mu\text{m}$ , 1.0  $\mu\text{m}$  and 0.5  $\mu\text{m}$  (Fig. 6).

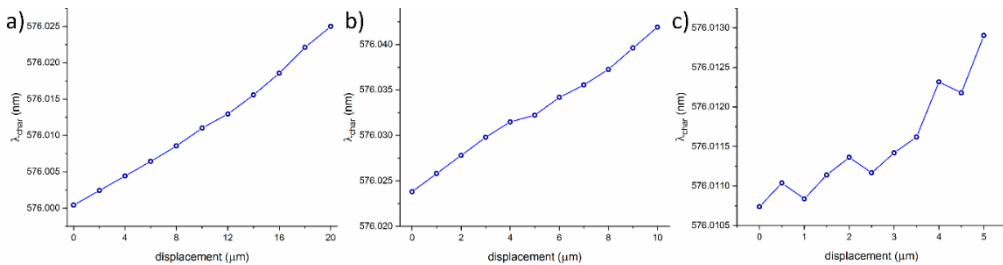


Fig. 6. Results of the experimental determination of the resolution in the case of using the Lorentz algorithm for different steps of the sample displacement: (a) 2.0  $\mu\text{m}$ , (b) 1.0  $\mu\text{m}$ , (c) 0.5  $\mu\text{m}$  (Zakrzewski et al., 2021)

For the 2.0  $\mu\text{m}$  displacement of the sample, the extracted  $\lambda_{\text{char}}$  values can be distinguished easily by the optical system. In this case, a practically linear relationship was obtained (Fig. 6a). Minor fluctuations occur for a displacement of 1.0  $\mu\text{m}$ , but the  $\lambda_{\text{char}}$  values are still distinguishable (Fig. 6b). For a displacement of 0.5  $\mu\text{m}$ , the tendency of the curve becomes "zigzag" and consequently the system loses the ability to determine the correct  $\lambda_{\text{char}}$  value. Taking into account the presented results, it was assumed that the resolution of the developed system is 1.0  $\mu\text{m}$ . The values of the optical system parameters determined on the basis of selected algorithms for three different measuring ranges are presented in the Table below (Table 1).

Table 1. The parameters of the optical system determined on the basis of experimental tests (Zakrzewski et al., 2021)

Parameter	Arg max			Gauss			Lorentz/Voigt		
	10	20	50	10	20	50	10	20	50
Measuring range (mm)	10	20	50	10	20	50	10	20	50
Trueness (mm)	0,081	0,102	0,943	0,022	0,051	0,913	0,009	0,052	0,921
Precision (mm)		0,022			0,003			0,002	
Accuracy (% of measuring range)	$\pm 1,04$	$\pm 1,06$	$\pm 1,93$	$\pm 0,25$	$\pm 0,27$	$\pm 1,83$	$\pm 0,11$	$\pm 0,14$	$\pm 1,84$
Resolution [mm]		0,004			0,001			0,001	
Linearity ( $R^2$ )	0,99977	0,99990	0,99914	0,99999	0,99996	0,99913	1	0,99997	0,99912

Regardless of the selected algorithm, the accuracy of the optical system decreases with the increase of the measuring range. The highest accuracy value ( $\pm 0.11\%$  of the measuring range) was obtained in the case of the  $\lambda_{\text{char}}$  extraction by Lorentz fit function. This value was obtained for a measuring range of 10 mm. Additionally, no difference in the results was observed between the  $\lambda_{\text{char}}$  extraction based on the Lorentz and Voigt functions. The materials commonly used in laser processing are characterized by different optical properties of the surface. Therefore, the system parameters were verified on an additional material, i.e. Ti6Al4V alloy. Consequently, a series of 3 measurements was carried out in selected measuring ranges and with a step of 1 mm. Additionally, the Lorentz function was chosen as the  $\lambda_{\text{char}}$  extraction algorithm because the best results were obtained for this method (Table 2).

Table 2. The accuracy of the optical system determined for 316L steel and Ti6Al4V alloy in the case of using the Lorentz algorithm.

Sample	Accuracy (% of measuring range)		
	10 mm	20 mm	50 mm
Ti6Al4V	$\pm 0.41$	$\pm 0.45$	$\pm 1.44$
316L	$\pm 0.49$	$\pm 0.49$	$\pm 1.63$

Finally, the system was validated in the off-line regime. For this purpose, a sample with a stepped change in height was produced from 316L steel. The theoretical thickness of each sample was 2 mm. Firstly, the prepared sample was measured using a Keyence LJ-V7060 laser triangulator with an accuracy of 0.4  $\mu\text{m}$ . Then, the sample was placed under the laser head integrated with the optical system. At each sample height (step), 5 measurements were carried out at random places. The  $\lambda_{\text{char}}$  values were determined using the Lorentz fit. Finally, the sample displacement resulting from the change in its height was calculated on the basis of the calibration curve obtained for the PSM (Fig. 5). The obtained results of measurements of the sample using the triangulator and the developed system are convergent (Fig. 7a). Additionally, the residues are within the range of the determined accuracy of the optical system (0.049 mm) for the 316L material (Fig. 7b).



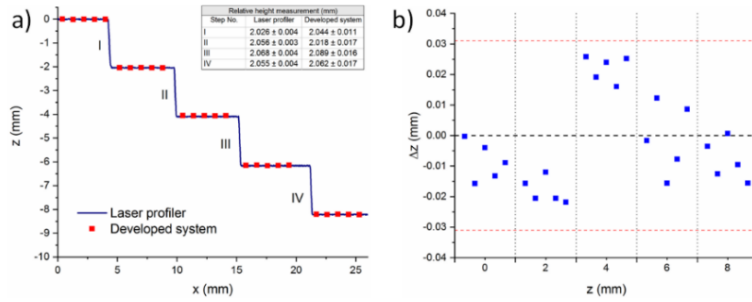


Fig. 7. (a) Results of sample measurement obtained with the laser triangulator and the developed system), (b) residual graph with the selected accuracy range (Zakrzewski et al., 2021)

#### 4. Application of the measurement system in the on-line regime

The effectiveness of the developed optical system was also analyzed on-line, i.e. during the laser processing of Ti6Al4V alloy. The local laser remelting process was carried out using a semiconductor generator with a maximum power of 4 kW and the BPP beam quality parameter of  $33 \text{ mm} \cdot \text{mrad}$ . The laser source was connected to the optical laser head by means of an optical fiber with a core diameter of  $1000 \mu\text{m}$ . The focal length of the process lens was 250 mm for  $\lambda_{\text{cen}}$ , and the laser beam had an almost perfect top hat power distribution ( $M2 = 150$ ). The signal acquired by the detector of the system operating in the off-line regime is shown on Fig. 8a. The  $\lambda_{\text{char}}$  value extracted by the modified Lorentz fitting algorithm corresponds to  $\lambda_{\text{cen}}$ . The modification included the analysis of only 50 spectral points from the value of the maximum peak intensity. Moreover, the process of laser remelting the material was carried out with a beam of 500 W (Fig. 8b) and 1000 W (Fig. 8c), respectively. Spectral signals in both modes were recorded 20 times with the same acquisition time and then averaged. Consequently, the extracted value of  $\lambda_{\text{char}}$  is identical during off-line and on-line operation of the optical system and corresponds to the value of  $\lambda_{\text{cen}}$ .

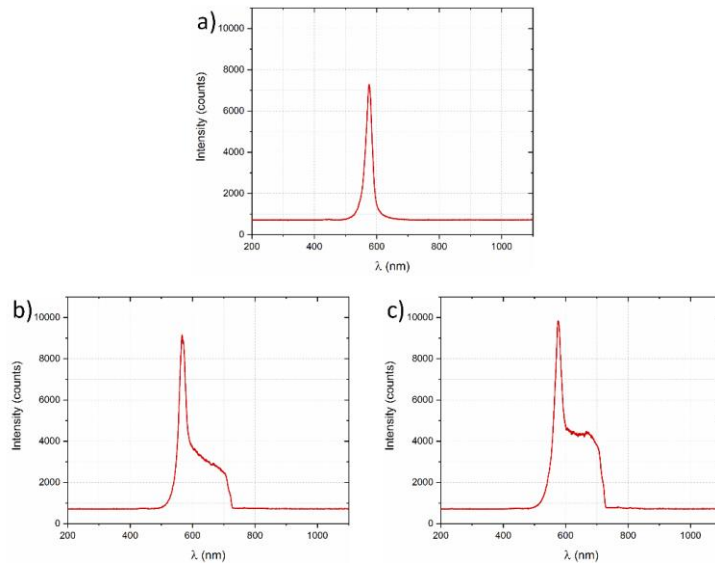


Fig. 8. The signal registered on the system detector in the following regimes: (a) off-line, (b) on-line with a beam power of 500 W, (c) on-line with a beam power of 1000 W

## 5. Conclusions

The workflow during development of confocal displacement sensor was deeply described with impact on the most important parts of the design process. It was shown that the selection of optical components can be carried out with defined quality factors influencing resultative aberration range (LCA), intensity, and FWHM. The approach for spectral data processing was presented as well as the results of implementing different fitting algorithms (Gauss, Lorentz and Voigt). In case of developed system the Lorentz algorithm was chosen as the one providing the smallest error. The full characterization of the measurement system for PSM material was described with additional consideration of materials typically used in LMD process. In both regimes (off-line and online) the developed systems showed correct functionality. The difference between results obtained in off-line regime with developed measurement system and triangulation system can be regarded as negligible. In case of system operation with laser switched on (on-line regime) the preliminary results show the validity of using the system in LMD process.

## Acknowledgements

This paper was supported by The National Centre for Research and Development, project No. LIDER/18/0071/L-9/17/NCBR/2018 "Process control of laser material processing using the phenomenon of chromatic aberration".

## References

- Accuracy (trueness and precision) of measurement methods and results, ISO 5725-1:1994.
- Asselin M., Toyserkani E., Iravani-Tabrizipour M., Khajopour A., Development of trinocular CCD-based optical detector for real-time monitoring of laser cladding, Proceedings of the IEEE International Conference on Mechatronics & Automation, pp. 1190-1196, Niagara Falls, Canada, 2005.
- Authier N., Baptiste A., Touvrey C., Bruyere V. and Namy P., Implementation of an interferometric sensor for measuring the depth of a capillary laser welding, Proceedings of the ICALEO Conference 2016, paper #904.
- DePond P.J., Guss G., Ly S. et al., In situ measurements of layer roughness during laser powder bed fusion additive manufacturing using low coherence scanning interferometry, Materials and Design 154(2018), pp. 347-359.
- Donadello S., Motta M., Demir A.G., Previtali B., Coaxial laser triangulation for height monitoring in laser metal deposition, Procedia CIRP 74(2018), pp. 144-148.
- Hu D., Kovacevic R., Sensing, modeling and control for laser-based additive manufacturing, International Journal of Machine Tools & Manufacture 43(2003), pp. 51-60.
- Huang W., Kovacevic R., A Laser-Based Vision System for Weld Quality Inspection, Sensors 11(2011), pp. 506-511.
- Leach R., Displacement measurement in Fundamental Principles of Engineering Nanometrology; Elsevier Science: Amsterdam, The Netherlands, 95-132 (2014).
- Luo D., Kuang C., and Liu X., Fiber-based chromatic confocal microscope with Gaussian fitting method," Opt. Laser Technol. 44 (2012), pp. 788-793.
- Mazumder J., Dutta D., Kikuchi N., Ghosh A., Closed loop direct metal deposition: art to part, Optics and Lasers in Engineering 34(2000), p. 397-414
- Neef A., Seyda V., Herzog D., Emmelmann C., Schönleber M., Kogel-Hollacher M., Low coherence interferometry in selective laser melting, Physics Procedia 56(2014), pp. 82-89.
- Song L., Bagaveth-Singh V., Dutta B., Mazumder J., Control of melt pool temperature and deposition height during direct metal deposition process, International Journal of Advanced Manufacturing Technologies 58(2012), pp. 247-256.
- Zakrzewski A., Jurewicz P., Koruba P., Ćwikła M., and Reiner J., Characterization of a chromatic confocal displacement sensor integrated with an optical laser head", Appl. Opt. 60(2021), pp. 3232-3241.

Zakrzewski A., M. Ćwikła M., Koruba P., Jurewicz P., and Reiner J., Design of a chromatic confocal displacement sensor integrated with an optical laser head, *Appl. Opt.* 59(2020), pp. 9108–9117.